Close-range exposure to a COVID-19 carrier: transmission trends in the respiratory tract and estimation of infectious dose

Saikat Basu[1,2,*]

[1]Department of Mechanical Engineering, South Dakota State University, Brookings, SD, USA
[2]Department of Otolaryngology / Head and Neck Surgery, The University of North Carolina at Chapel Hill – School of Medicine, Chapel Hill, NC, USA
[*]saikat.basu@sdstate.edu / saikat_basu@med.unc.edu

How respiratory physiology and airflow therein proceed to impact SARS-CoV-2 transmission, leading to the initial infection, is an open question. An answer can help determine the susceptibility of an individual on exposure to a COVID-2019 carrier and can also quantify the still-unknown *infectious dose* for the disease. Combining computational fluid mechanics-based tracking of respiratory transport in anatomic domains with sputum assessment data from hospitalized patients and earlier measurements of ejecta size distribution during regular speech – this study shows that targeted deposition at the initial nasopharyngeal infection sites peaks over the droplet size range of 2.5 – 19 μ, and reveals that the number of virions that can establish the infection is at most of $\mathcal{O}(\mathbf{10^2})$.

Severe acute respiratory syndrome coronavirus 2 (SARS-CoV-2) has been identified as the causative agent for coronavirus disease 2019 (COVID-19), that has inflicted a global pandemic with almost 16 million confirmed infections and exceeding 640,000 deaths worldwide (as of late-July 2020).[1]

As is well-known by now, transmission of respiratory infections such as COVID-19 occurs through carriage of pathogens via droplets of different sizes produced during sneezing, coughing, singing, normal speech, and even, breathing.[2] Accordingly, the means of person-to-person infection are projected to be three-way[3]: (a) inhalation of virus-laden droplets emitted by an infected individual at close-range; (b) inhalation of vaporized droplet nuclei that can float in air for hours; and (c) contaminating the respiratory mucosa through physical contact to external surfaces (*fomites*) with droplet deposits sitting on them. While (a) is valid for short-distance exposures to the COVID-19 carrier, transmission through modes (b) and (c) can happen over larger distances and longer time scales. However, clustering trends of infection spread (e.g. in industrial units[4], in closed groups[5], and inside households[6]) suggest that close-range exposures can be a critical determinant in worsening the pandemic. A follow-up question might be – *what entails an exposure?* A key component therein are the respiratory droplet sizes one is exposed to. Coughing and sneezing typically generate droplets with length-scales of $\mathcal{O}(10^2)$ to $\mathcal{O}(10^3)$ μ, while oral droplets ejected during normal speaking can range over $\sim 0.1 - 500$ μ.[3,7] The main competing effects determining the fate of these droplets are the ambient temperature and humidity (e.g. low relative humidity induces fast evaporation and shrinkage of the droplets), and the size of the droplet that controls its inertia and the gravitational force acting on it. While smaller droplets would stay airborne for longer, the larger droplets tend to fall fast ballistically; with the critical size for this transition being in the vicinity of 100 μ.[8,9] Of note here, this study does not insist on any nomenclatural distinction between "aerosols" and "droplets" owing to ambiguities[10] in common perception, and simply refers to all expiratory liquid particulates as *droplets*.

For mechanistic tracking of what range of virus-bearing droplet sizes might be more potent for transmission and to eventually induce infection, it is key that we identify the initial infection sites. A recent study[11] used SARS-CoV-2 isolates to examine and compare the infection process of cultured cells from different parts of the human airway. The data reveals a striking pattern of continuous variation from a relatively high infectivity in ciliated epithelial cells along the nasal passage lining, to less infectivity in cells lining the throat and bronchia, and finally to relatively low infectivity at the lung cells. The pattern is governed through angiotensin-converting enzyme 2 (ACE2), which is a single-pass type I membrane protein and is the cell surface receptor that the virus utilizes to intrude into cells. ACE2 is abundant on ciliated epithelial cells, but is relatively scarce on the surface of the lower airway cells. While the findings are for *in vitro* samples, deposition of virus-laden droplets along the anterior nasal airway might not be so effective as to launch an infection despite the presence of ciliated cells, since the mucus layer provides some protection against virus invasion and infection.[3] This leaves out the nasopharynx (the region along the respiratory tract posterior to the septum and comprising the upper part of the pharynx, see Panel A in Figure 1) as the main initial infection site; it acts as the seeding zone for subsequent infection of the lower airway via aspiration of virus-laden boluses of nasopharyngeal fluid. The *ansatz* is supported by data[12] on the efficacy of nasopharyngeal swab testing for COVID-19 diagnosis, when compared to oropharyngeal swabs. So at this point, a valid question to ask would be: *what are the typical droplet sizes that are making their way to the nasopharynx during inhalation?*

Respiratory droplets, on being expelled, undergo dehydration and consequent shrinkage, the extent of which partially depends on the fraction of non-volatile material in the droplets, e.g. dehydrated epithelial cell remnants, white blood cells, enzymes, DNA, sugars, electrolytes etc. So, although sputum is 99.5% water; ejected droplets, on dehydration, would have

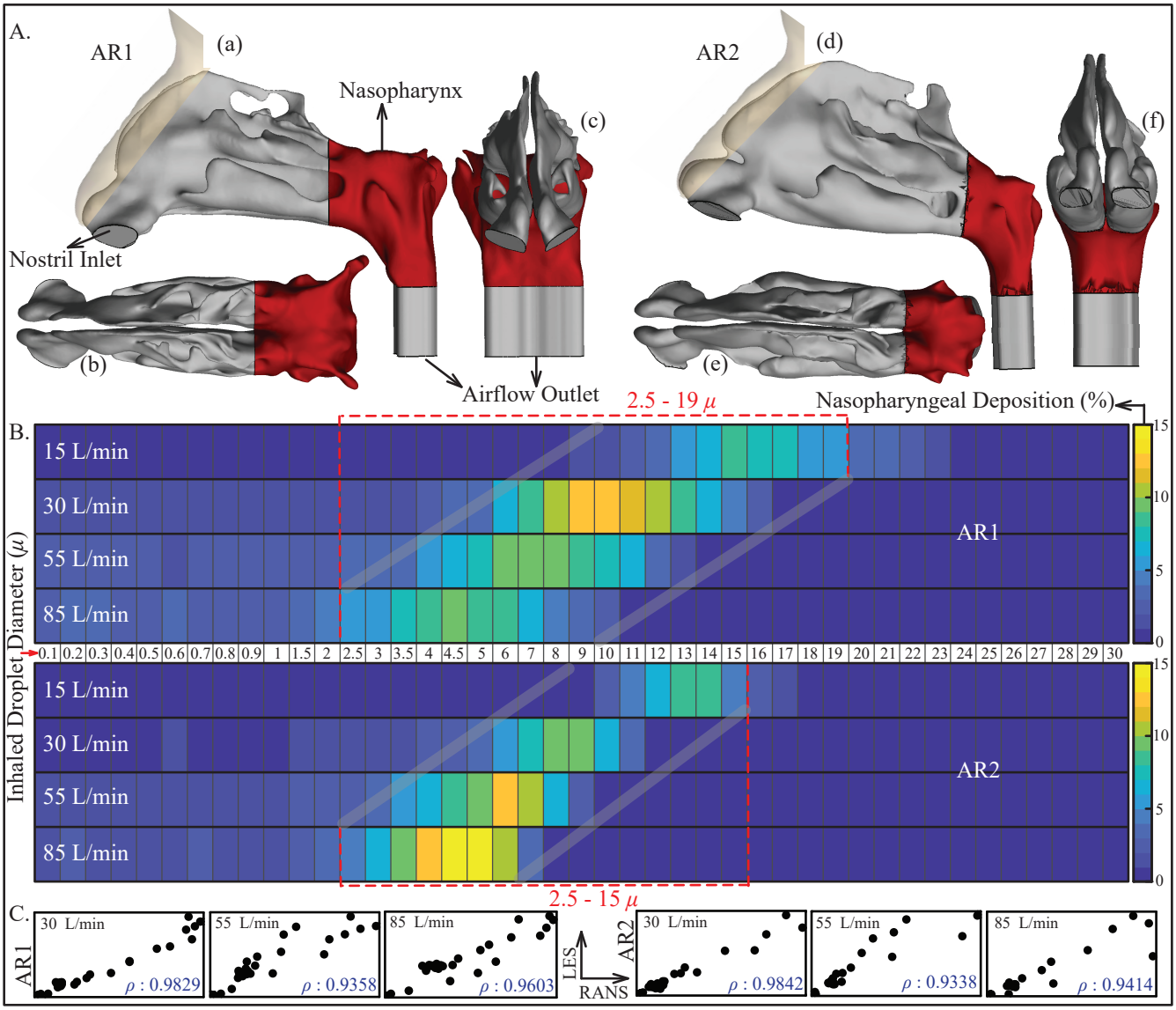

Figure 1. A. The sagittal, axial, and coronal views of the CT-based nasal domains, shown respectively in a–c for anatomic reconstruction 1 (AR1) and d–f for anatomic reconstruction 2 (AR2). Nasopharynx is marked in red. **B.** Visuals of heat-maps for inspiratory transmission trends, showing the percentage of droplets of each size undergoing nasopharyngeal deposition (NPD). Data for different inhaled airflow rates are arranged along separate rows. Tracked droplet sizes are along the horizontal axis (positioned between the two heat-maps for AR1 and AR2). NPD peaks for droplets sized between 2.5 – 19 μ in AR1 and 2.5 – 15 μ in AR2. **C.** Correlation between RANS-based SST k-ω and LES results for the higher airflow rates i.e. 30, 55, and 85 L/min; therein the first three frames (bottom-left) are for AR1, the other three frames (bottom-right) are for AR2. The frames have an aspect ratio of 0.5; ρ represents the Pearson's correlation coefficient.

a higher density of 1.3 g/ml,[13] which is what has been used for droplet tracking simulations here. This considers that the non-volatile weight fraction is in the 1 – 5% range. Such dehydration shrinks the expelled droplet diameter to 27 – 34% of the initial size. Therefore, assuming a mean 30% shrinkage and considering 100 μ as the critical size that prompts ballistic sedimentation, this study tracks inhaled droplet sizes in the range of 0.1 μ to 30% of 100 μ, i.e. 30 μ, for close-range exposure. The choice of the minimum in the size range, i.e. 0.1 μ, is dictated by SARS-CoV-2 size, which is in between 0.08 – 0.2 μ, with an average physical diameter of 0.1 μ.[14]

Next piece in this puzzle comprises the breathing parameters. Allometric relations[15] approximate the minute inhalation at 18.20 L/min for a 75-kg male and 15.05 L/min for a 75-kg female, for gentle steady breathing while sitting awake. In general, the inspiratory flow rates can stretch over a wide range of ∼15 – 85 L/min, based on whether the individual is inhaling gently or sniffing. This study tests droplet transmission at four different inhalation rates, viz. 15, 30, 55, and 85 L/min; notably these discrete flow rates are the ones traditionally used in literature[16] to gauge filtration capacities of protective mask respirators. Flow physics undergo a transition over this

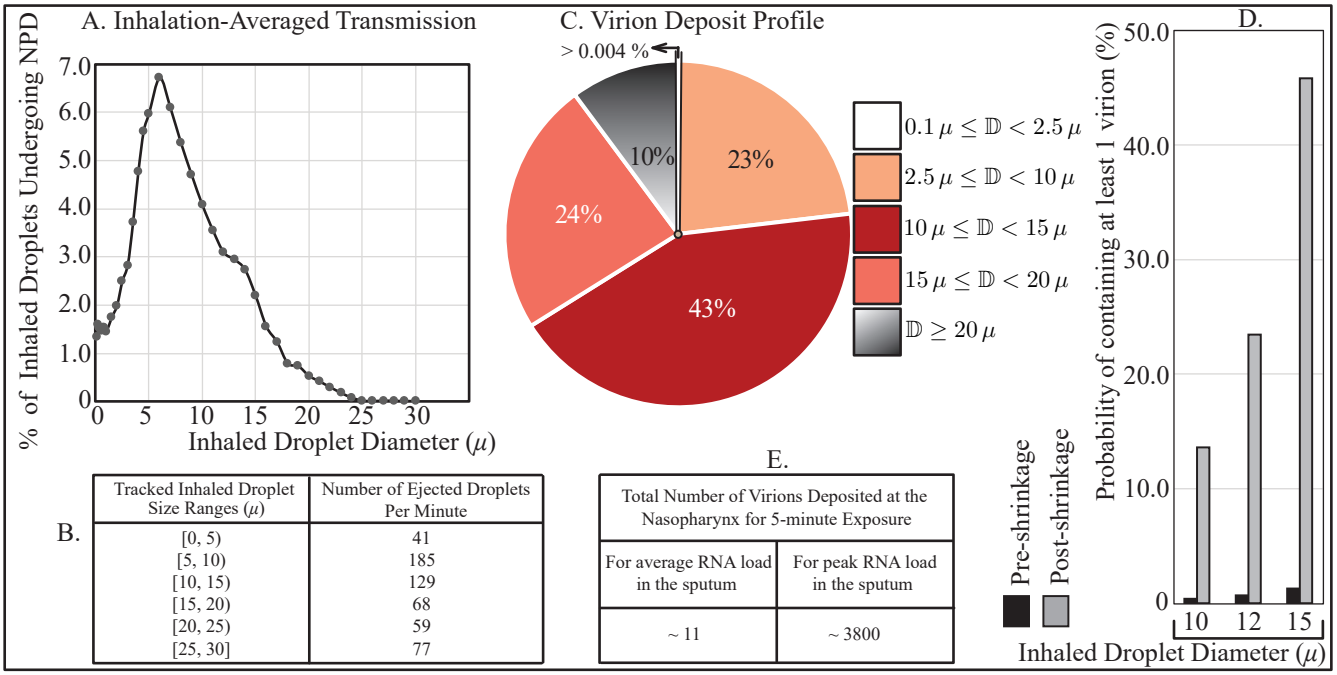

B.

Tracked Inhaled Droplet Size Ranges (μ)	Number of Ejected Droplets Per Minute
[0, 5)	41
[5, 10)	185
[10, 15)	129
[15, 20)	68
[20, 25)	59
[25, 30]	77

E.

Total Number of Virions Deposited at the Nasopharynx for 5-minute Exposure	
For average RNA load in the sputum	For peak RNA load in the sputum
~ 11	~ 3800

Figure 2. A. Graphical representation of the percentage of droplets of each size undergoing deposition at the nasopharynx; averaged from AR1 and AR2, for the tested inhalation rates. **B.** Distribution of droplet sizes ejected each minute during normal speaking, the numbers are calculated from earlier studies on expelled droplet tracking with food coloring.[9] **C.** Pie diagram showing which droplet sizes are dominant contributors for virion transmission at the nasopharynx, for ejecta size distribution as in panel **B**. Symbol $\mathbb{D}$ is the inhaled droplet diameter. The numbers assume that the droplets have undergone dehydration before being inhaled into the nasal airspace. **D.** Probabilistic interpretation of a droplet to contain at least 1 virion, based on whether the droplet size at inhalation is pre-dehydration or post-dehydration. **E.** Estimated number of virions that are deposited at the susceptible individual's nasopharynx via dehydrated inhaled droplets, during close-range exposure to a COVID-19 carrier.

range; e.g. the 15 L/min flow through anatomically realistic nasal conduits lies in the laminar regime, the flow structures however devolve into turbulence at higher inhalation rates. Numerical schemes, that are used to track respiratory transport, have been selected accordingly (see the supplementary methods section). Note that with nasopahrynx being the initial infection zone, inhaled transport via mouth poses less likely for virion transmission and the modeling framework focuses on the nasal domain.

Computed tomography (CT) scans of the nasal airway from two healthy adult subjects were used in this study, to develop: anatomic reconstruction 1 (AR1) and 2 (AR2). Refer to the methods, for details of the *in silico* geometry building. Note that while it might be possible to access many research scans with some form of sinonasal irregularity, as they make part of disease-specific studies; it is relatively rare to have nasal scans from otherwise healthy subjects and hence limits the size of this study's test cohort. For unbiased conclusions, it is, however, critical that we use disease-free CT-normal nasal airway domains to track the virion transport characteristics that would lead to the infection.

The overall droplet size range of 2.5 – 19 μ (in AR1: 2.5 – 19 μ, in AR2: 2.5 – 15 μ) registers the peak, in terms of the percentage of droplets of each size that are deposited at the nasopharynx. The range is determined by a cut-off of at least 5% deposition for around 3000 tracked droplets (viz. 3015 in AR1, 3000 in AR2) of each size. Panel B in Figure 1 lays out the heat-maps for nasopharyngeal deposition (NPD) for different droplet sizes, at the four tested inhaled airflow rates. The discrete droplet sizes that are tracked are along the horizontal axis of the heat-maps. The patch bounded by the grey lines can be a definitive marking technique to delineate the hazardous droplet size range for airborne transmissions. Note that this finding assumes that the post-dehydration density of the respiratory droplets is at 1.3 g/ml. If there is little or no dehydration and as such the expelled droplet density remains at ~1 g/ml, the droplet size range for peak NPD upscales to 3 – 20 μ; since the lighter droplets can now penetrate further into the airspace, the transport being aided by the ambient inspiratory streamlines.

During a real exposure to a COVID-19 carrier, the vulnerable individual can be considered to inhale at different rates over the duration of exposure. Panel A in Figure 2 extracts the averaged nasopharyngeal deposition for the different tested inhalation rates in the two subjects. Such inhalation-averaged transmission presents an approximate droplet size range of 2.5 – 15.0 μ for a minimum 2% NPD for each droplet size.

The next pertinent question is: *how effective are these droplets at carrying virions?* SARS-CoV-2 belongs to a family of single-stranded RNA viruses, and virological assessments[17] done on the sputum of hospitalized COVID-19 patients show an averaged viral load of 7×10^6 RNA copies/ml

of oral fluid, with the peak load being 2.35×10^9 copies/ml. For the average load, simple calculations (see methods) show that the probability that a dehydrated 10-μ droplet (contracted from its original size of ~ 33 μ) will carry at least 1 virion is 13.6%. The same number is 45.8% for a post-shrinkage 15-μ droplet. The probability drops exponentially to 0.2% for a 2.5-μ dehydrated droplet. Now, with existing data on the size distribution of expelled droplets during normal speaking (see Panel B, Figure 2), the proportion of virion deposits at the nasopharynx by different droplet sizes can be computed (see Panel C, Figure 2) using the transmission data presented in Figure 1. Conspicuously enough, in the absence of dehydration, the probability of 1 virion in, for instance, a 10-μ droplet plummets to 0.37% (see Panel D, Figure 2). This rationalizes why in geographic regions with high humidity (and hence less dehydration and shrinkage of respiratory ejecta), the pandemic's spread has been relatively slow.[18]

Finally, the *infectious dose* is a fundamental virological measure quantifying the number of virions that can go on to start an infection; the value of which is still not conclusively known for SARS-CoV-2.[19] Theoretically, according to the *independent action hypothesis*,[20] even a single virion can potentially establish an infection in highly susceptible systems. Whether the hypothesis is true for humans and specifically for SARS-CoV-2 transmission is as yet undetermined. The rapid spread of COVID-19 though *a priori* suggests a small infective dose for the disease, that is ameliorating person-to-person transmission.

Since it is unethical to expose subjects to SARS-CoV-2 (especially in the current absence of a remediating therapeutic – as of July 2020), this study introduces a strategy synergizing computational tracking and virological data, to quantify the infectious dose. Based on the nasopharyngeal transmission trends (Figure 1) and the virion transmission data (Panels B-C of Figure 2), for a 5-minute exposure: the number of virions depositing at the susceptible individual's nasopharynx is 11 (considering average RNA load in the carrier's sputum). If the infecting individual is in more serious stage of morbidity and hence considering the peak RNA load, as many as 3835 virions will be deposited on the nasopharynx of the exposed individual over 5 minutes (see Panel E in Figure 2). Now for a rough estimate of infectious dose, consider the March 2020 Skagit Valley Chorale superspreading incident[5] where an infected person transmitted the disease to 52 other individuals in a 61-member choir group. The exposure time at the incident was reported to be 2.5 hours; consequently, for an average RNA load (assuming that the carrier was having mild-to-moderate symptoms), the number of virions depositing at a closely-positioned susceptible individual's nasopharynx over that duration approximates to $(11/5) \times 2.5 \times 60 \approx 330$. So, ~ 300 can be considered a conservative upper estimate for the COVID-19 infective dose, the order agreeing with preliminary estimates from replication rates of the virus.[21]

That the number of virions needed to establish the infection is at most of $\mathcal{O}(10^2)$ is indeed remarkable! The scale manifests how communicable this disease is, especially if discerned in the perspective of infectious doses for other airborne transmissions, e.g. the infective dose for influenza A virus, when administered through aerosols to human subjects lacking serum neutralizing antibodies, ranges between 1950 – 3000 virions.[22] The discovery, together with this study's detection of droplet sizes that target the infection-prone nasopharynx, could provide a useful resource in mitigating the COVID-19 pandemic and in the design of topical anti-viral therapeutics and targeted intra-nasal vaccines that can induce prophylaxis through mucosal and systemic immune responses.

Methods

Anatomic geometry reconstruction

Medical imaging-based *in silico* model generation was accomplished according to relevant guidelines and regulations, with the anatomic geometries being reconstructed from existing de-identified imaging data of two CT-normal subjects. The use was approved with exempt status by the Institutional Review Board at UNC Chapel Hill. The test subjects include a 61 year-old female (AR1) and a 37 year-old female (AR2). The nasal airspaces were extracted from the medical grade scans (with the CT slices collected at coronal depth increments of ~ 0.4 mm) over a delineation range of -1024 to -300 Hounsfield units, and was complemented by careful hand-editing of the selected pixels to ensure anatomic accuracy. For this step, the DICOM (Digital Imaging and Communications in Medicine) scans for each subject were imported to the image processing software Mimics 18.0 (Materialise, Plymouth, Michigan).

The reconstructed geometries were imported as stereolithography files to ICEM-CFD 15.0 (ANSYS, Inc., Canonsburg, Pennsylvania), and then meshed spatially into minute volume elements. As per mesh refinement-based protocols[23], each grid comprised more than 4 million unstructured, graded tetrahedral elements (e.g. 4.54 million in AR1, 4.89 million in AR2); along with three prism layers of 0.1-mm thickness at the airway walls, with a height ratio of 1. The nostril inlet planes comprised 3015 elements in AR1 (1395 elements in left nostril, 1620 elements in right nostril) and 3000 elements in AR2 (1605 in left nostril, 1395 in right nostril).

Numerical simulations

The study considers droplet transport for four different inhaled airflow rates, viz. 15, 30, 55, and 85 L/min. The lower flow rate (i.e. 15 L/min) corresponds to comfortable resting breathing, with the viscous-laminar steady-state flow physics model standing in as a close approximation.[24,25] At higher flow rates (extreme values of which may sometimes lead to nasal valve collapse), the shear layer separation from the tortuous walls of the anatomic geometries results in turbulence. To track that, the study averages the droplet deposition percentages from implementation of two distinct categories of numerical schemes, viz. (a) shear stress transport (SST) based k-ω model, which is a sub-class under Reynolds-averaged Navier Stokes (RANS)

schemes that parameterize the action of all turbulent fluctuations on to the mean flow; and (b) Large Eddy Simulation (LES). The two numerical techniques show high correlation in terms of droplet deposition at the nasopharynx (see Figure 1, Panel C). However, it should be noted that while the SST k-ω scheme, a 2-equation eddy-viscosity model, is computationally less expensive; it averages the short time-scale flow artifacts, such as the short-lived vortices, that might emerge in these complicated domains; and hence the prediction of droplet transport affected by the simulated ambient airflow may at times contain errors. LES is computationally more expensive, it separates the turbulent flow into large-scale and small-scale motions, and accounts for the small fluctuations through a sub-grid scale model (in this study, Kinetic Energy Transport Model was used as the sub-grid scale model[26]). We take the averaged estimates of NPD from the two schemes, to minimize statistical and algorithmic biases.

The computational schemes employed a segregated solver on ANSYS Fluent, with SIMPLEC pressure-velocity coupling and second-order upwind spatial discretization. Solution convergence was monitored by minimizing the flow residuals (viz. mass continuity $\sim \mathscr{O}(10^{-4})$, Cartesian velocity components $\sim \mathscr{O}(10^{-5})$), and through stabilizing the mass flow rate and static pressure at the airflow outlets. For the pressure-driven airflow simulations: typical convergence run-time for a laminar simulation with 5000 iterations was approximately 5–6 hours for 4-processor based parallel computations executed at 4.0 GHz speed. The corresponding run-time for a RANS simulation was $\sim$ 12 hours; for an LES computation, it was 4–5 days. Note that for the LES work, the simulated flow time was 0.5 sec for the 30 L/min case, with 0.0002 sec as the time-step[27] and it was 0.25 sec for the 55 and 85 L/min flow rates with the time-step at 0.0001 sec. $\rho = 1.204$ kg/m^3 was used as air-density, and $\mu = 1.825 \times 10^{-5}$ kg/m.s was assumed as air's dynamic viscosity.

Following set of boundary conditions were enforced during the simulations: (i) zero velocity at the airway-tissue interface i.e. at the walls enclosing the nasal airspace (otherwise commonly referred to as the *no slip* condition), along with "trap" boundary condition for droplets whereby a droplet would come to rest after depositing on the walls; (ii) zero pressure at nostril planes, which were the pressure-inlet zones in the simulations, with "reflect" boundary condition for droplets to mimic the effect of inhalation on the droplet trajectories if they are about to fall out of the anterior nasal domain; and (iii) a negative pressure at the airflow outlet plane, which was the pressure-outlet zone, with "escape" boundary condition for droplets, i.e. allowing for the outgoing droplet trajectories to leave the upper respiratory airspace. Mean inlet-to-outlet pressure gradients were -9.01 Pa at 15 L/min, -26.65 Pa at 30 L/min, -73.73 Pa at 55 L/min, and -155.93 Pa at 85 L/min. For a reference on the general layout of the anatomic regions, see Panel A in Figure 1.

On convergence of the airflow simulations, inhaled droplet dynamics were tracked through Lagrangian-based discrete phase particle transport simulations in the ambient airflow; with the localized deposition along the airway walls obtained through numerically integrating transport equations that consider contribution of the airflow field on the evolution of droplet trajectories, along with the effects for gravity and other body forces such as the Saffman lift force that is exerted by a flow-shear field on small particulates moving transverse to the streamwise direction. Also, the droplet size range is considered large enough to discount Brownian motion effects on their spatial dynamics. Note that the study tracked 3015 droplets of each size in AR1 and 3000 droplets of each size in AR2, the numbers being same as the number of elements on the nostril inlet planes which were seeded with the to-be-tracked droplets for the droplet transport simulations. Post-processing of the droplet deposition data along the airway walls provides the nasopharyngeal deposits. This numerical protocol has been rigorously validated[28] by comparing the deposition trends along the inner walls of similar *in silico* digital models to the *in vitro* spray tests carried out in 3D-printed solid replicas of the same reconstructions.

Probabilistic estimation of virion contamination in expiratory droplets

Suppose the viral load in a COVID-19 carrier has been assessed to be $\mathscr{V}$ copies of RNA in each ml of sputum fluid. Let a typical expelled droplet diameter from the carrier be $\mathbb{D}$ μ. With SARS-CoV-2 being a single-stranded RNA virus, the average number of virions in each droplet can then be computed as $(\pi/6)\mathscr{V}\mathbb{D}^3 \times 10^{-12}$. Therefore, every 100 droplets of the same size would have $(\pi/6)\mathscr{V}\mathbb{D}^3 \times 10^{-10}$ virions; which, in other words, also represents the probability (in %) for a droplet of diameter $\mathbb{D}$ μ, of containing at least 1 virion.

References

1. Johns-Hopkins-University. Coronavirus Resource Center. Web link (accessed 25-July-2020).
2. Bourouiba, L. Turbulent gas clouds and respiratory pathogen emissions: potential implications for reducing transmission of COVID-19. *JAMA* **323**, 1837–1838 (2020).
3. Mittal, R., Ni, R. & Seo, J. H. The flow physics of COVID-19. *J. Fluid Mech.* **894** (2020).
4. Dyal, J. W. COVID-19 Among Workers in Meat and Poultry Processing Facilities - 19 States, April 2020. *MMWR. Morb. mortality weekly report* **69** (2020).
5. Miller, S. L. *et al.* Transmission of SARS-CoV-2 by inhalation of respiratory aerosol in the Skagit Valley Chorale superspreading event. *medRxiv* (2020).
6. Li, W. *et al.* The characteristics of household transmission of COVID-19. *Clin. Infect. Dis.* (2020).
7. Xie, X., Li, Y., Sun, H. & Liu, L. Exhaled droplets due to talking and coughing. *J. Royal Soc. Interface* **6**, S703–S714 (2009).

8. Wells, W. F. On airborne infection: study II, droplets and droplet nuclei. *Am. J. Epidemiol.* **20**, 611–618 (1934).

9. Xie, X., Li, Y., Chwang, A. T. Y., Ho, P. L. & Seto, W. H. How far droplets can move in indoor environments - revisiting the Wells evaporation-falling curve. *Indoor Air* **17**, 211–225 (2007).

10. Resnick, B. The debate over "airborne" coronavirus spread, explained. Web link (accessed 25-July-2020).

11. Hou, Y. J. *et al.* SARS-CoV-2 Reverse Genetics Reveals a Variable Infection Gradient in the Respiratory Tract. *Cell* (2020).

12. Patel, M. R. *et al.* Performance of oropharyngeal swab testing compared to nasopharyngeal swab testing for diagnosis of COVID-19 - United States, January-February 2020. *Clin. Infect. Dis.* (2020).

13. Stadnytskyi, V., Bax, C. E., Bax, A. & Anfinrud, P. The airborne lifetime of small speech droplets and their potential importance in SARS-CoV-2 transmission. *Proc. Natl. Acad. Sci.* **117**, 11875–11877 (2020).

14. Bar-On, Y. M., Flamholz, A., Phillips, R. & Milo, R. Science Forum: SARS-CoV-2 (COVID-19) by the numbers. *Elife* **9**, e57309 (2020).

15. Garcia, G. J. M. *et al.* Dosimetry of nasal uptake of water-soluble and reactive gases: a first study of interhuman variability. *Inhalation Toxicol.* **21**, 607–618 (2009).

16. He, X., Reponen, T., McKay, R. T. & Grinshpun, S. A. Effect of particle size on the performance of an N95 filtering facepiece respirator and a surgical mask at various breathing conditions. *Aerosol Sci. Technol.* **47**, 1180–1187 (2013).

17. Wölfel, R. *et al.* Virological assessment of hospitalized patients with COVID-2019. *Nature* **581**, 465–469 (2020).

18. Wang, J., Tang, K., Feng, K. & Lv, W. High temperature and high humidity reduce the transmission of COVID-19. *Available at SSRN 3551767* (2020).

19. Lakdawala, S. & Gaglia, M. What We Do and Do Not Know About COVID-19's Infectious Dose and Viral Loads. Web link (accessed 25-July-2020).

20. Zwart, M. P. *et al.* An experimental test of the independent action hypothesis in virus–insect pathosystems. *Proc. Royal Soc. B: Biol. Sci.* **276**, 2233–2242 (2009).

21. Wang, D. *et al.* Population Bottlenecks and Intra-host Evolution during Human-to-Human Transmission of SARS-CoV-2. *bioRxiv* (2020).

22. Nikitin, N., Petrova, E., Trifonova, E. & Karpova, O. Influenza virus aerosols in the air and their infectiousness. *Adv. Virol.* **2014** (2014).

23. Frank-Ito, D. O., Wofford, M., Schroeter, J. D. & Kimbell, J. S. Influence of mesh density on airflow and particle deposition in sinonasal airway modeling. *J. Aerosol Medicine Pulm. Drug Deliv.* **29**, 46–56 (2016).

24. Basu, S., Frank-Ito, D. O. & Kimbell, J. S. On computational fluid dynamics models for sinonasal drug transport: Relevance of nozzle subtraction and nasal vestibular dilation. *Int. J. for Numer. Methods Biomed. Eng.* **34**, e2946 (2018).

25. Kimbell, J. S. *et al.* Upper airway reconstruction using long-range optical coherence tomography: Effects of airway curvature on airflow resistance. *Lasers Surg. Medicine* **51**, 150–160 (2019).

26. Baghernezhad, N. & Abouali, O. Different SGS models in Large Eddy Simulation of 90° square cross-section bends. *J. Turbul.* N50 (2010).

27. Ghahramani, E., Abouali, O., Emdad, H. & Ahmadi, G. Numerical investigation of turbulent airflow and microparticle deposition in a realistic model of human upper airway using LES. *Comput. & Fluids* **157**, 43–54 (2017).

28. Basu, S. *et al.* Numerical evaluation of spray position for improved nasal drug delivery. *Sci. Reports* **10**, 1–18 (2020).

29. Basu, S. COVID-19 anatomic CFD data. Link to Google Drive folder (online; available from 23-July-2020).

Acknowledgements

This material is based upon work supported by the National Science Foundation (NSF), under Award Number 2028069 for COVID-19 research. Any opinions, findings, and conclusions or recommendations expressed here are those of the author and do not necessarily reflect NSF's views. Supplemental support came from SB's faculty start-up package at SDSU.

The author acknowledges Adam J Kimple, MD, PhD (attending rhinologist at the Department of Otolaryngology/Head & Neck Surgery, UNC CH), Leonardo P Chamorro, PhD (at the Department of Mechanical Science & Engineering, UIUC), and Sunny Jung, PhD (at the Department of Biological & Environmental Engineering, Cornell University) for many fruitful discussions. Acknowledgements are also due to Julia S Kimbell, PhD (at the Department of Otolaryngology/Head & Neck Surgery, UNC CH) for mentoring and support. Computing facilities at both SDSU and UNC CH were used for the work.

Author contributions statement

SB designed the study, performed research, analyzed the data, and drafted the manuscript.

Data availability

This project has generated simulated quantitative, de-identified data on regional deposition along nasal tissues. The datasets (including Fluent .cas, .dat files) and the numeric protocols; along with MATLAB codes, Wolfram Mathematica notebooks, and Microsoft Excel spreadsheets used for data post-processing – are available from the corresponding author on request, through a shared-domain Google Drive folder[29].

Additional information

The author declares no competing interests.

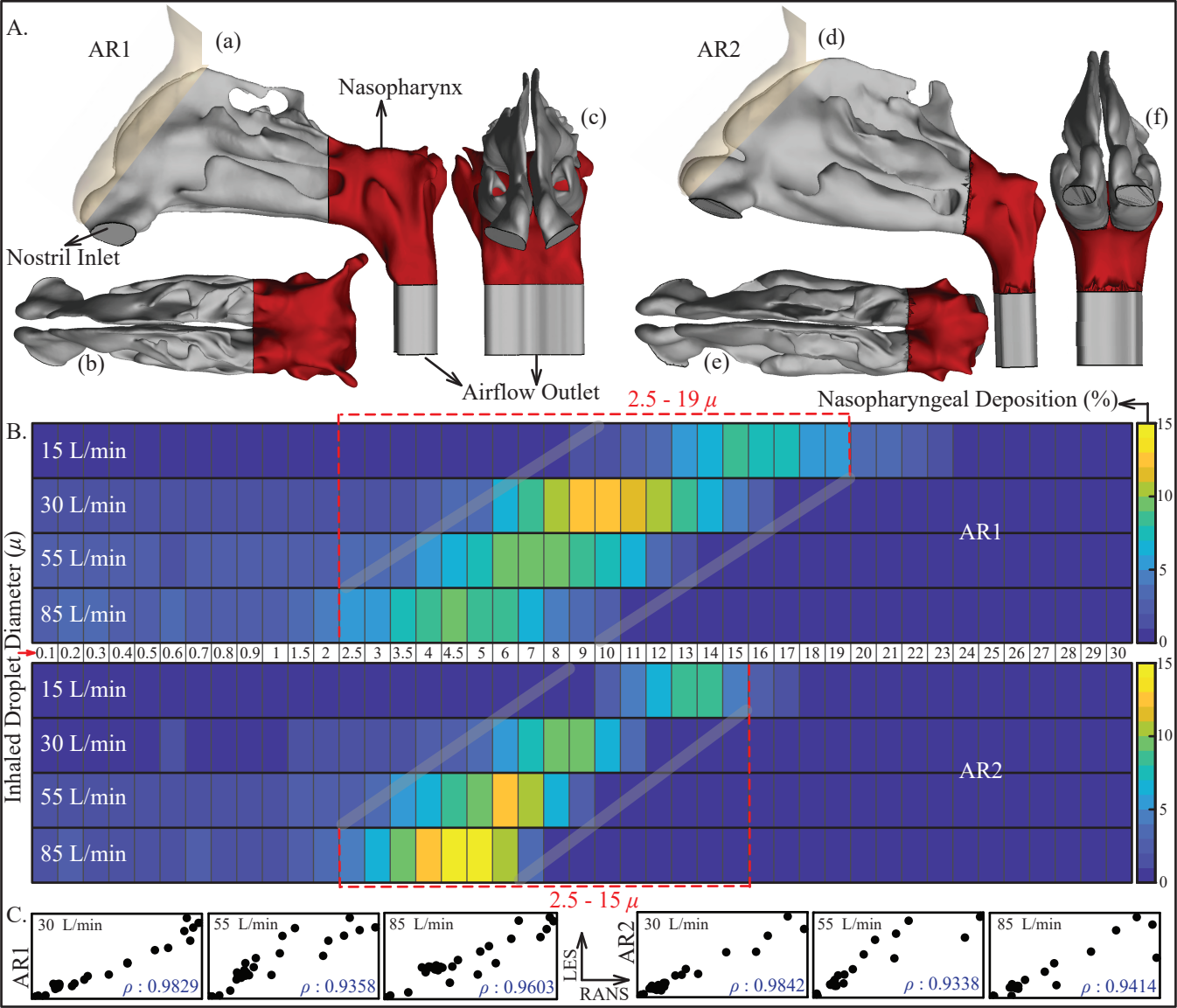
A.
AR1
(a)
Nasopharynx
(c)
Nostril Inlet
(b)
Airflow Outlet
AR2
(d)
(f)
(e)
2.5 - 19 μ
Nasopharyngeal Deposition (%)
B.
15 L/min
30 L/min
55 L/min
85 L/min
AR1
Inhaled Droplet Diameter (μ)
0.1 0.2 0.3 0.4 0.5 0.6 0.7 0.8 0.9 1 1.5 2 2.5 3 3.5 4 4.5 5 6 7 8 9 10 11 12 13 14 15 16 17 18 19 20 21 22 23 24 25 26 27 28 29 30
15 L/min
30 L/min
55 L/min
85 L/min
AR2
2.5 - 15 μ
15
10
5
0
C.
AR1
30 L/min
ρ : 0.9829
55 L/min
ρ : 0.9358
85 L/min
ρ : 0.9603
LES
RANS
AR2
30 L/min
ρ : 0.9842
55 L/min
ρ : 0.9338
85 L/min
ρ : 0.9414

A. Inhalation-Averaged Transmission

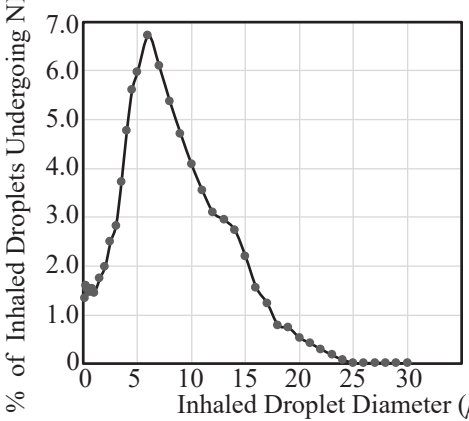

C. Virion Deposit Profile

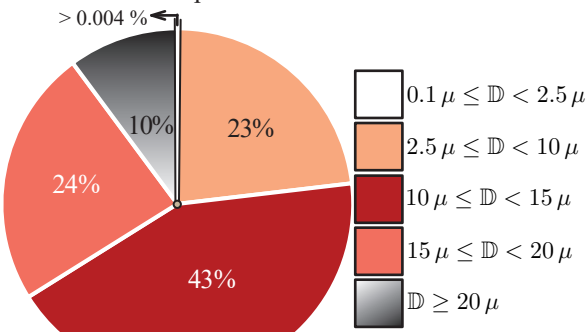

D.

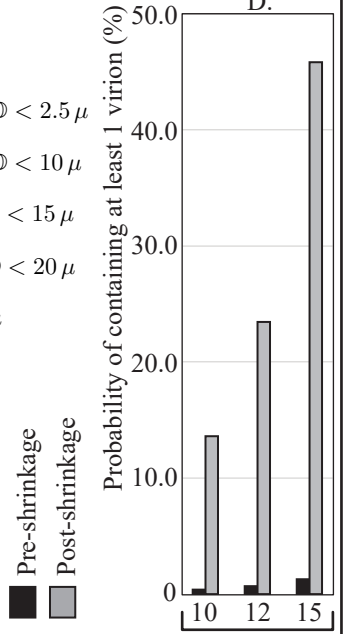

B.

Tracked Inhaled Droplet Size Ranges (μ)	Number of Ejected Droplets Per Minute
[0, 5)	41
[5, 10)	185
[10, 15)	129
[15, 20)	68
[20, 25)	59
[25, 30]	77

E.

Total Number of Virions Deposited at the Nasopharynx for 5-minute Exposure	
For average RNA load in the sputum	For peak RNA load in the sputum
~ 11	~ 3800